Silicon (2022) 14:6611–6620
https://doi.org/10.1007/s12633-021-01410-y

ORIGINAL PAPER

Halloysite Nanotubes (HNTs)-Filled Ethylene-Propylene-Diene Monomer/Styrene-Butadiene Rubber (EPDM/SBR) Composites: Mechanical, Swelling, and Morphological Properties

P. Sendil Ganeche[1] · P. Balasubramanian[1] · S. Vishvanathperumal[2]

Received: 30 June 2021 / Accepted: 20 September 2021 / Published online: 9 October 2021

Abstract
Halloysite nanotubes (HNTs) were incorporated into an EPDM/SBR rubber/styrene-butadiene rubber (SBR) composite by melt blending of HNTs into the EPDM/SBR blend. The mechanical properties, abrasion and swelling resistance of HNTs ranging from 2 parts per hundred rubber (phr) to 10 parts per hundred rubber (phr) were investigated in EPDM/SBR base rubber. Tensile strength, 100% modulus (modulus at 100% elongation), elongation at break and tear strength were evaluated at ambient temperature using electric universal tensile testing equipment in accordance with ASTM D-412. Hardness, abrasion and swelling resistance were determined using Shore-A Durometer, DIN abrader and immersion techniques, respectively. The results show that increasing HNT content increased tensile strength, tear strength, hardness (stiffness), and crosslink density. The surface morphology of tensile-fractured material was studied using field-emission scanning electron microscopy (FE-SEM). According to FE-SEM results, the most roughness of the surface was seen at HNTs filled rubber nano-composites.

Keywords EPDM/SBR · HNTs · Mechanical properties · Swelling resistance

1 Introduction

Polymers are lightweight, have a high specific strength/modulus, are easy to process, and are inexpensive [1]. Without some kind of reinforcement, a rubber substance, whether polar or non-polar, has weak physico-mechanical properties [2]. The addition of a number of ingredients with special roles, such as curatives (activator, catalyst, and vulcanization or cross-linking agents), aids in the enhancement of those properties. At the present days, rubber and curatives materials are well-known and are not becomes an issue to any further extent. However, many academicians and researchers have recently improved the problem of modifying or replacing traditional additives such as carbon black (CB) and silica [3–5]. Because of their unique particle form and hydrophobic surface, CB is recommended as a strong reinforcement particle with better dispersibility in rubber matrix [6]. In addition, CB particle caused pollution in atmosphere and displayed dark color in the composite [7, 8]. Due to its hydrophilic surface, silica is recognised as a white filler with similar reinforcement effect as CB and low dispersion in rubber matrices, which appears in natural rubber (NR) composite [6, 9]. As a result, a variety of researchers [10–14] have introduced new types of nano-fillers, such as clay particles, to enhance the mechanical and swelling properties of rubber composites. They are also layered silicates and belong to the phyllosilicate group, which includes montmorillonite, saponite, and hectorite. Silica, which is commonly used as a rubber reinforcing filler, is a non-carbon filler [15, 16], with usage second only to carbon black in the rubber reinforcing industry. The presence of many hydroxyl groups on the surface of silica, on the other hand, causes filler tendentious aggregation, which is unfavourable to rubber composite performance.

Carbon nanotubes (CNTs) are divided into single-walled carbon nanotubes (SWCNTs), which have a typical diameter of 1–2 nm, and multi-walled carbon nanotubes (MWCNTs),

✉ P. Sendil Ganeche
sendilganeche@gmail.com

[1] Department of Mechanical Engineering, A.V.C College of Engineering, Mayiladuthurai - Akkur Road, Mannampandal, Mayiladuthurai, Tamil Nadu 609305, India

[2] Department of Mechanical Engineering, S.A. Engineering College, Poonamallee, Avadi Road Veeraraghavapuram, Thiruverkadu, Tamil Nadu 600077, India

which have an outer diameter of 3–30 nm or more, depending on the number of graphitic layers comprising their structure [17]. CNTs also have a low mass density and a large aspect ratio (length to diameter ratio of approx 1000) [18]. Mechanical (elastic modulus: 1–1.7 TPa), thermal (thermal conductivity greater than 3000 $W{\cdot}m^{-1}{\cdot}K^{-1}$), and electrical (electrical conductivity: 10^5 $S{\cdot}m^{-1}$ – $10^7{\cdot}S{\cdot}m^{-1}$) properties are all outstanding [19]. Carbon nanotubes, while their enormous benefits, have a few disadvantages. CNTs have a great inclination to aggregate due to their nanometric size. Carbon nanotubes are also rather costly [20, 21]. Natural halloysite nanotubes are another sort of nanotubular structure (HNTs). HNTs have been found to be effective as nanofillers in a variety of rubber materials [22, 23]. HNTs are a two-layered aluminosilicate ($Al_2Si_2O_5(OH)_4$. H_2O) with a hollow tubular structure in the micron range and chemically similar to kaolin particles [24, 25]. HNTs are a type of phyllosilicates material that consists of one octahedral sheet and one tetrahedral sheet with six-membered rings and 1:1 layers. The crystalline structure of HNTs is double layered. The outer layer surface of HNTs has Si-O groups, while the inner side surface and tube edges have $Al(OH)_3$- groups [26]. HNTs have a higher aspect ratio than clay minerals (montmorillonite, saponite, and hectorite) due to their tuber shape. HNTs have an aspect ratio ranging from 10 to 130, depending on the tube dimension. HNTs' large surface area and aspect ratio are likely to have a unique reinforcing impact on the polymer matrix. For nanocomposites to improve their mechanical and thermal properties, good interaction and interfacial adhesion between the rubber matrix and nano-filler particles are essential [7]. The lengths of HNTs typically range from 300 to 1500 nm, with inner diameters of 15–100 nm and outside diameters of 40–120 nm [27, 28]. HNTs are a low-cost, environmentally acceptable substance that can be disseminated in a polymer matrix more easily than carbon nanotubes [29]. Because of the fact that HNTs materials are naturally occurring and much cheaper, yet structurally comparable to MWCNTs, the HNTs could be a best choice for more expensive CNTs for some applications. EPDM, SBR, and silicone rubber can all endure temperatures as low as −40 degrees Celsius, making them ideal for low-temperature applications. Both materials have the same degree of compression set, making them suitable for applications requiring a high level of durability. EPDM and SBR have high tensile strength and abrasion resistance, making them ideal materials for dynamical loading and force applications that require a lot of physical effort [30, 31].

The addition of HNTs to the EPDM/SBR matrix results in a new material. Because of the high aspect ratio and low density, HNTs nanofiller materials combine the features of matrix and filler, and may also display additional properties. Nano-reinforcement has been the focus of recent nanocomposites manufacturing research in order to produce improved or tailored mechanical performance. This usually refers to gaining some unique tensile qualities, as well as abrasion and swelling resistance, in the case of nano-reinforcements. This work is an important accountability in the creating of new material of EPDM/SBR nanocomposites filled with various contents of HNTs. The objective of this paper is to explain the reinforcing ability of EPDM/SBR nanocomposites on the mechanical and swelling properties.

2 Experimental

2.1 Materials

Sigma-Aldrich supplied the halloysite nanotubes (HNTs) and swelling chemicals. The HNTs had a relative density of 2.53 g/cm^3 and a basic surface area of 65 m^2/g. The tubes had a diameter of 40–80 nm and a length of 1 to 4 μm. Arihant Reclamation Private Limited, Delhi, India, provided ethylene-propylene-diene monomer (EPDM) rubber (KEP-270; Mooney viscosity 71 ML_{1+4}, 125 °C; ENB content 4.5 wt.%; ethylene content 57 wt.%, volatile content 0.4 wt.%; specific gravity 0.86) and styrene-butadiene rubber (SBR-1502; bound styrene 23.5 wt.%; volatile matter 0.3 wt.% ash 0.2 wt.%; organic acid 5.8 wt.%; specific gravity 0.94; Mooney viscosity 52 ML_{1+4}, 100 °C). The zinc oxide and stearic acid used as activator, sulphur used as vulcanizing agent, tetramethylthiuram disulfide (TMTD) and mercaptobenzothiazyl disulfide (MBTS) used as accelerator and was purchased from Sigma-Aldrich. Without any further purification, all chemicals were utilised as received.

2.2 Preparation of Nanocomposites

In an open mill mixer, EPDM rubber, styrene-butadiene rubber (SBR), Halloysite nanotubes (HNTs), and other ingredients (zinc oxide, stearic acid, tetramethylthiuram disulfide (TMTD), mercaptobenzothiazyl disulfide (MBTS), and sulphur) were mixed together (50 °C). The friction ratio is maintained in mixer is 1:1.4. Stage 1: Before mixing, rubber was passed 9–10 times between the mill rollers having a less than 1 mm nip gap. Stage 2: After homogenization of both the rubber (i.e., EPDM and SBR), the other ingredients like activator (zinc oxide and stearic acid), accelerator (TMTD and MBTS), and curing agent (sulphur) were added according to Table 1. For preparing various samples of EPDM/SBR blends, the amount of HNTs were different proportion as shown in Table 1. A semi-automated electrically powered hydraulic press was used to shape the composites sheet with a thickness of 2 mm. At a pressure of 30 MPa, the press temperature was held at 160 °C for a 10 min cure time.

Table 1 Formulation of EPDM/SBR-HNTs Compounds

Sample code	Compounds (phr)							
	EPDM	SBR	HNTs	Zinc oxide	Stearic acid	MBTS	TMTD	Sulphur
H_0	80	20	0	4	1.5	1.2	1	2.5
H_2	80	20	2	4	1.5	1.2	1	2.5
H_4	80	20	4	4	1.5	1.2	1	2.5
H_6	80	20	6	4	1.5	1.2	1	2.5
H_8	80	20	8	4	1.5	1.2	1	2.5
H_{10}	80	20	10	4	1.5	1.2	1	2.5

2.3 Testing and Characterization of Rubber Composites

EPDM/SBR nanocomposites were tested for tensile properties (tensile strength, elongation at break, and modulus) according to ASTM D-412. At ambient temperature, the tensile properties were calculated using a Universal Testing Machine (UTM) model Dak System Inc., T-72102, series 7200 with a crosshead speed of 500 mm/min. The tear strength is also measured in the same machine and conduction as per ASTM D-624 [10]. The hardness of the composites has been performed as per ASTM D-2240 by the Shore-A Durometer hardness tester. The abrasion characteristics of the rubber composite were measured using a DIN abrader according to ASTM D-5963 and are expressed in terms of volume loss. The swelling resistance was measured using the ASTM D-471 immersion process [12]. At different temperatures of 30 °C, different penetrates such as aromatic, aliphatic, and chlorinated hydrocarbons are used to analyse the swelling properties of the composites. The mole percent uptake was calculated by this Eq. (1)

$$Q_t(mol\%) = \frac{(M_t - M_0)/MW}{M_0} \times 100 \quad (1)$$

where, M_t = Final mass of the composite,

M_0 = Initial mass of the composite.

MW = Molecular weight of the penetrate.

The following eq. (2) [32–34] was used to measure the degree of crosslinking density:

$$\vartheta\left(\frac{mol}{cm^3}\right) = \frac{1}{2M_c} \quad (2)$$

where, M_c = Molar mass of the polymer between crosslinks.

The Flory-Rehner eq. (3) was used to measure the molar mass between the crosslinks of the composites [32–35]:

$$M_c\left(\frac{g}{mol}\right) = \frac{-\rho_p V_s V_r^{1/3}}{\ln(1-V_r) + V_r + \chi V_r^2} \quad (3)$$

where, ρ_p = Polymer Density,

V_s = Molar volume of the solvent (106.3 mL/gmol),

V_r = Volume fraction of the solvent-swollen filled polymer compound,

χ = Interaction parameter of the polymer (0.3) [36], and.

V_r can be determined by the following eq. (4) [37]:

$$V_r = \frac{1}{1 + Q_m} \quad (4)$$

where, Q_m = Weight swell of the composites in toluene.

The tensile fractured surface of composites were observed with a Sigma with Gemini Column, CARL ZEISS FE-SEM, USA at the acceleration voltage of 10 kV. The specimen surfaces were coated with gold with thickness of 10–20 nm.

3 Results and Discussion

Figure 1 depicts the stress-strain curves of EPDM/SBR-HNTs nanocomposites. The addition of 2 phr of HNTs to an EPDM/SBR blend resulted in stresses of roughly 8.15 MPa, a 33% increase over the base EPDM/SBR blend, whereas the addition of 10 phr of HNTs to an EPDM/SBR blend led in a

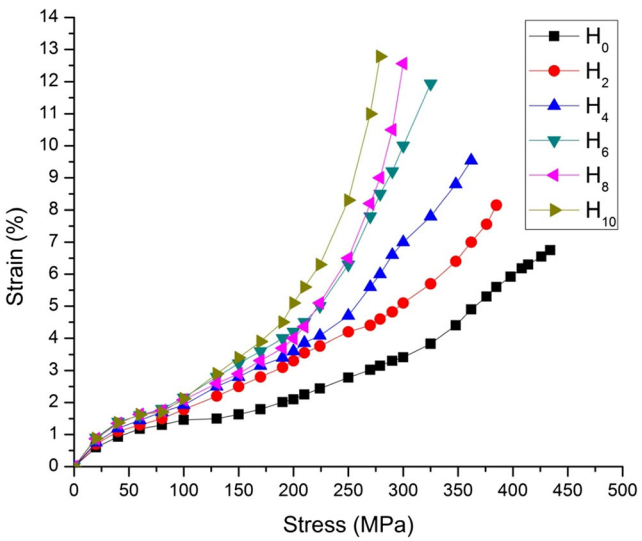

Fig. 1 Stress-strain curve of the EPDM/SBR-HNTs composites

stress of 12.78 MPa, a 109% increase over the base EPDM/SBR blend. Furthermore, because to the increased discontinuity in the rubber composite material, the addition of HNTs has reduced the strain % of EPDM/SBR-HNTs composites. Figures 2, 3, 4, 5, 6, and 7 show the mechanical properties of EPDM/SBR-HNTs nanocomposites, with information of mechanical properties such as tensile strength, 100% modulus, elongation at break, tear strength, hardness, and abrasion resistance. From Fig. 2, it is observed that the tensile strength of base rubber is very low strength, which is ineffective in practical application and is why desires to be incorporated by nano-materials. The addition of HNTs to EPDM/SBR-HNTs nanocomposites will increase their tensile strength. When the addition of HNTs is about 10 phr, the tensile strength of rubber nanocomposites is about 109% of that of base rubber blends. Furthermore, as the content of HNTs increased from 0 to 6 phr, the tensile strength increased rapidly due to better dispersion of nano-particles within the EPDM/SBR rubber matrix, and from 8 to 10 phr due to poor interaction, lesser agglomeration, and bonding between HNTs and EPDM/SBR matrix, which is responsible for the slight improvement in HNTs and rubber properties. As a result, the rubber-filler interfacial region's reinforcing effect of HNTs becomes extremely effective in influencing the tensile strength of EPDM/SBR-HNTs nanocomposites, resulting in increased tensile strength.

Figure 3 shows the modulus with different proportions of HNTs, calculated at 100% elongation. Figure 3 shows that as the HNTs loading in the EPDM/SBR composites increased, the modulus calculated at 100% elongation increased. The modulus at 100% elongation was used to determine the stiffness of the rubber composite. The 100% modulus was primarily influenced by the surface area, scale, and structure of HNTs. As a result, the composite with 6 phr of HNTs had a higher degree of cross-linking (as shown by the crosslinking density test), resulting in a higher 100% modulus. Since the composites filled with a higher amount of HNTs had a lower degree of chemical cross-linking, as shown by the cross-link density property in Fig. 8, the composites filled with a higher amount of HNTs had lower values. Low structural integrity, which is a significant parameter that can affect the characteristics of HNTs' reinforcing capacity, is also a result of high HNTs material. As a result, when compared to higher amounts of HNTs, the reinforcing impact of HNTs was reduced. The moduli were mostly impacted by the structure and surface area. EPDM/SBR composites filled with 8 phr of HNTs had a 3% decrease in modulus compared to EPDM/SBR composites filled with 6 phr of HNTs filler. However, because a change in modulus frequently has negative effects for applications, the reduced modulus is regarded as a positive.

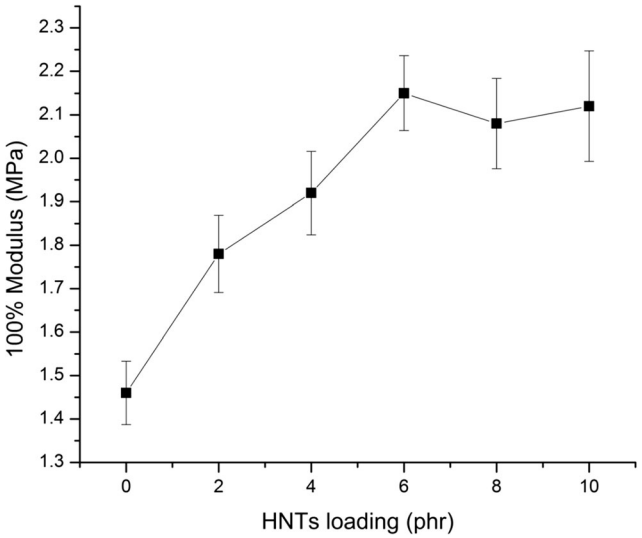

Fig. 3 100% modulus of the EPDM/SBR-HNTs composites

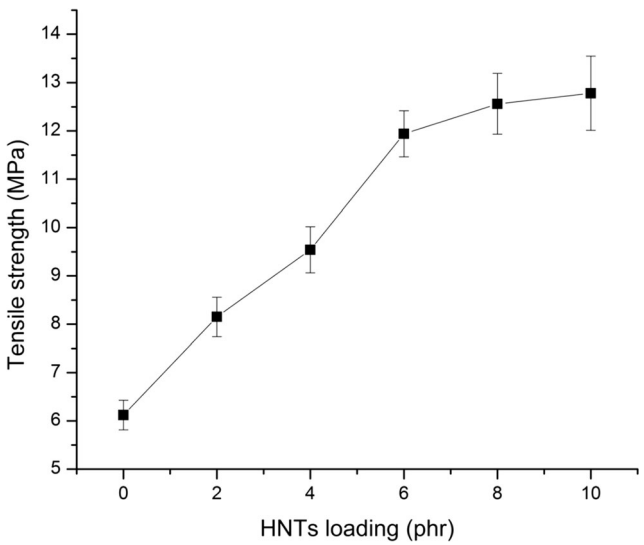

Fig. 2 Tensile strength of the EPDM/SBR-HNTs composites

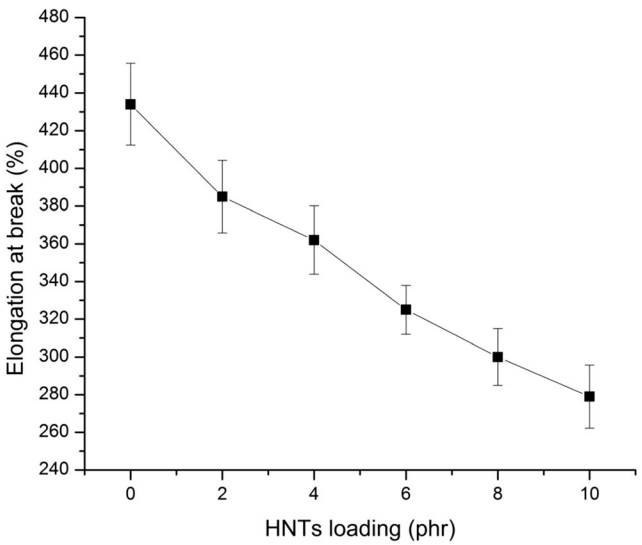

Fig. 4 Elongation at break of the EPDM/SBR-HNTs composites

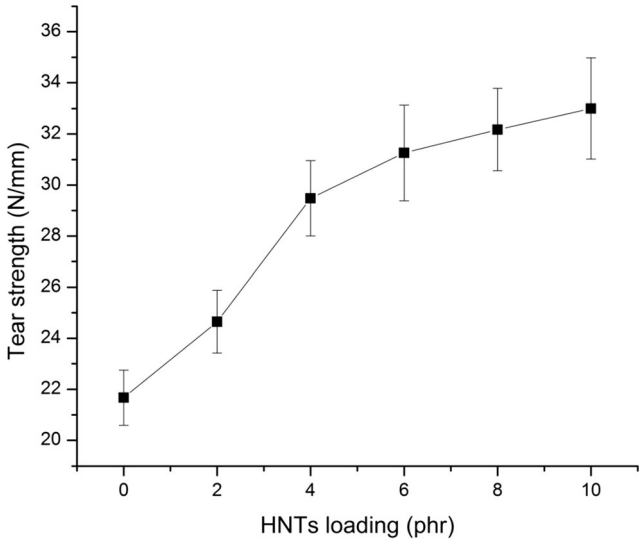

Fig. 5 Tear strength of the EPDM/SBR-HNTs composites

The effect of HNT loading on elongation at break is depicted in Fig. 4. With the addition of HNTs to the EPDM/SBR composites, the elongation at break decreased. The inter-tubular and interfacial bonding between the HNTs and the EPDM/SBR rubber matrix, as well as the better contact of the HNTs within the rubber matrix, play a key role in reducing the elongation at break. The improved interactions between the nano-filler and the rubber matrix increased the composites' strength and stiffness, reducing their ductility.

Figure 5 shows that as the HNTs were increased, the tear strength of the EPDM/SBR composites increased. The high crosslinking density of the HNTs-loaded composites was responsible for the steady increase in tear strength with the inclusion of HNTs in the composite. As a result, it can be inferred that HNTs inhibited crack propagation, thereby increasing the composites' resistance. As a result, HNTs with high structural integrity have a fair resistance to crack propagation.

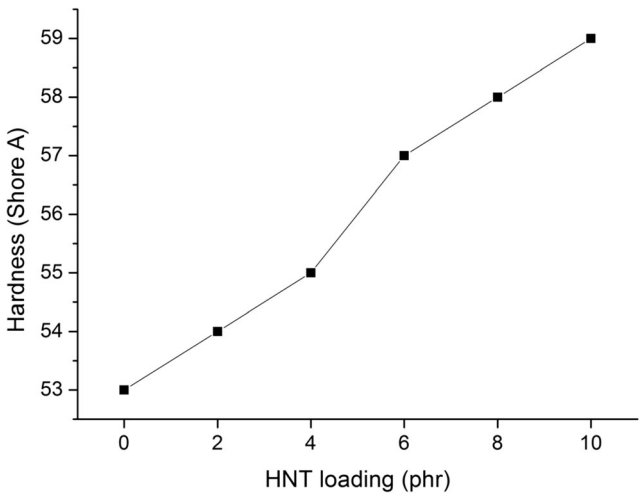

Fig. 6 Hardness of the EPDM/SBR-HNTs composites

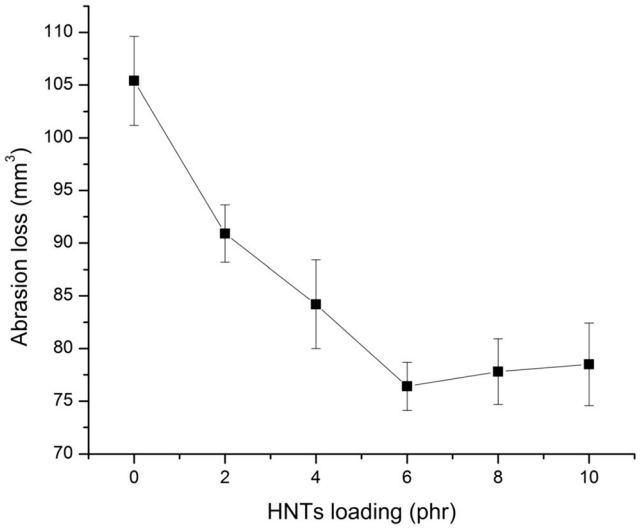

Fig. 7 Abrasion loss of the EPDM/SBR-HNTs composites

The mechanical property of rubber composites that is most significant is their hardness. Figure 6 illustrates the hardness of EPDM/SBR-HNT composites. The hardness of the composites varies depending on the amount of HNTs present. It begins at 53 Shore-A for unloaded compounds and steadily increases as the amount of HNTs in the HNTs nanofiller filled EPDM/SBR composites increases. The degree of crosslinking has a significant effect on the hardness of a compound. Furthermore, the HNTs' lower active surface area may have increased cross-links, which increased the composites hardness. The mechano-chemical grafting of EPDM/SBR molecular chains on the HNTs surfaces and the stretching orientation of HNT in EPDM/SBR-HNTs composites may be responsible for the enhancement of characteristics.

The abrasion loss of EPDM/SBR composites reinforced with HNTs is shown in Fig. 7. The abrasion resistance increases as the content of HNTs increases. This is due to the reinforcing effect of HNTs, which resulted in a stronger

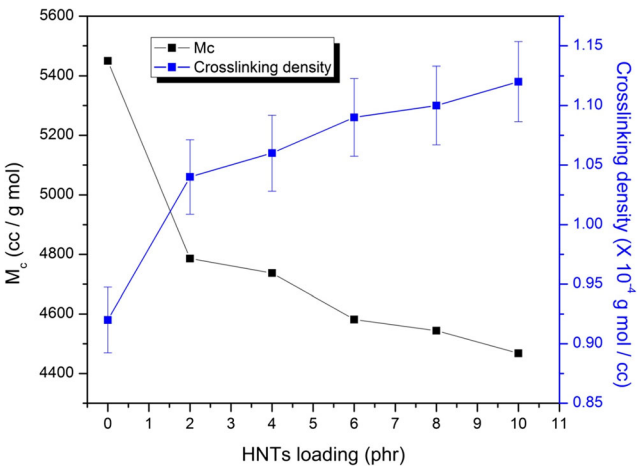

Fig. 8 Molecular weight of the polymer between the crosslinks (M_c) and crosslinking density of the EPDM/SBR-HNTs composites

rubber-filler network. Furthermore, increasing the crosslinking density made the composites stiffer and more abrasion resistant.

The mole percent uptake of the rubber composites in different solvent (aromatic, aliphatic and chlorinated) at 30 °C are shown in Table 2. The mole percent uptake was considerably decreased for HNTs reinforced composites as compared to neat EPDM/SBR blends. The higher HNT reinforcement in the EPDM/SBR rubber matrix limits the swelling-induced expansion of the rubber chains. This makes it very difficult for the solvent to penetrate the gaps between the rubber molecules, lowering the mole percent uptake. Hence, the rubber blend composites have higher solvent barrier properties compared to neat EPDM/SBR blends. The trend was in the order of: dichloromethane > chloroform > benzene > toluene > xylene > mesitylene > n-pentane > n-hexane > carbon tetrachloride > n-heptane > n-octane. The higher molecular weight of solvent exhibited the lowest absorption and vice-versa. From the Table 2, mole percent uptake trend was in order of: chlorinated > aromatic > aliphatic.

The crosslinking density was calculated by the help of equilibrium swelling measurement. A sample dimension about 250x250x2 mm was cut from the rubber sample. To assess the cross-linking density, EPDM/SBR composites were soaked in toluene for three days at 23 °C, with the toluene being replaced with new solvent (toluene) every day. An immersion test is performed to examine the nanofiller-rubber matrix interaction. Figure 8, shows the molecular weight of the polymer between the crosslinks (M_c) and crosslinking density of EPDM/SBR blend composites with different proportion of HNTs. The obtained result shows an increasing trend in crosslinking density after loading the HNTs. The crosslinking density is determined in part by the molecular weight of the polymer between the crosslinks (M_c). The M_c values of HNTs filler filled EPDM/SBR nanocomposites are lower than those of unfilled EPDM/SBR nanocomposites. With increased HNTs content, the molar mass between crosslinks (Mc) decreased. The accessible volume between consecutive crosslinks reduced as the Mc values declined. As the amount of HNTs in the EPDM/SBR-HNTs nanocomposites increased, the crosslinking density also increased. Tensile strength, tear strength, hardness, and abrasion resistance are all improved by increasing crosslinking density.

The FE-SEM micrograph of the fractured tensile surface are shown in Fig. 9 (a) HNTs Fig. 9 (b) EPDM/SBR blends, (c) EPDM/SBR composites containing 6 phr HNTs and (d) EPDM/SBR composites containing 10 phr HNTs. The image of HNTs is shown in Fig. 9 (a), showing the tube-like dimension and the nature of the tubes. It can be concluded that the tensile fractured morphology surface of unfilled EPDM/SBR was relatively smooth (Fig. 9 (b)). For EPDM/SBR reinforced with 10 phr composite, the tensile fractured surface exhibited notable undulating stripes and rough characteristics (Fig. 9 (d)). In comparison, the tensile fractured surface of EPDM/SBR reinforced with 6 phr HNT shows large deformation and many tear folds (Fig. 9(c)), and no noticeable curatives (zinc oxide, stearic acid, sulphur, etc) particles were observed, showing excellent compatibility and good interfacial bond strength between HNTs and EPDM/SBR compound due to the

Table 2 Mole percent uptake for different penetrant of composites material at 30 °C

Sample code	Mole percent uptake (mol%)										
	Aromatic				Aliphatic				Chlorinated		
	Benzene	Toluene	Xylene	Mesitylene	n-pentane	n-hexane	n-heptane	n-octane	Dichloromethane	Chloroform	Carbon tetrachloride
H_0	3.95	3.57	3.46	3.03	2.42	2.34	2.28	2.24	5.42	4.56	2.26
H_2	3.65	3.28	2.71	2.46	2.16	2.02	1.95	1.87	4.86	4.17	1.94
H_4	3.63	3.25	2.67	2.39	2.03	1.98	1.81	1.756	4.62	4.17	1.86
H_6	3.59	3.17	2.63	2.36	1.96	1.95	1.83	1.72	4.56	4.08	1.75
H_8	3.58	3.14	2.65	2.35	2.04	1.92	1.86	1.8	4.54	4.03	1.87
H_{10}	3.52	3.09	2.59	2.28	1.92	1.87	1.78	1.74	4.42	3.86	1.76

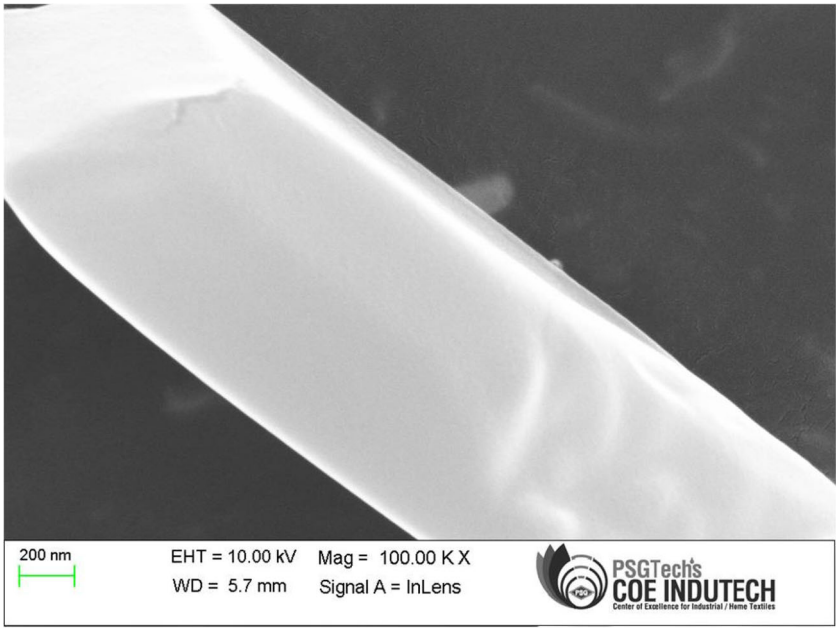

(a) HNT nanofiller

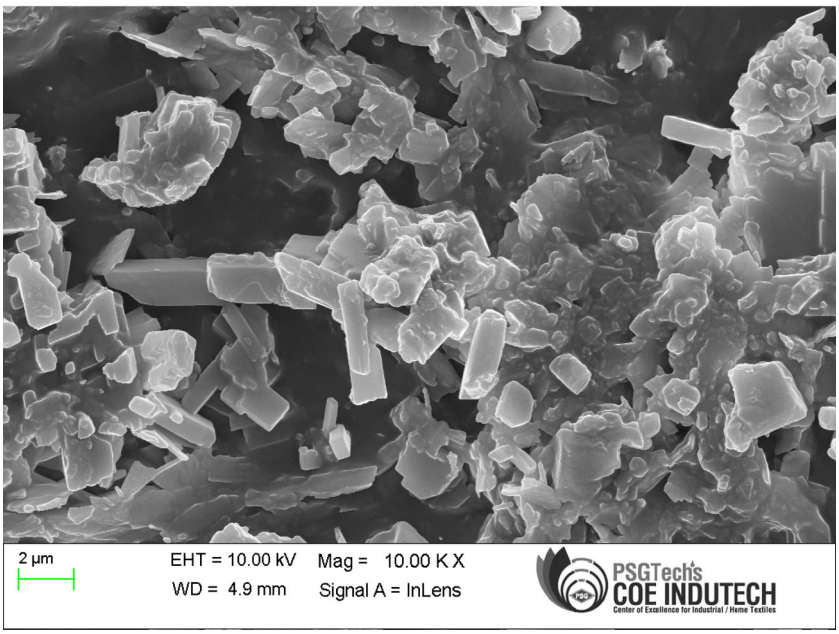

(b) EPDM/SBR blends

Fig. 9 The tensile fractured surfaces of EPDM/SBR-HNTs composites

SiO_2-Al_2O_3 present in the HNTs filler, which was reliable with the improved tensile strength of the composite.

4 Conclusions

EPDM/SBR with various HNT loadings was prepared in this research, tensile properties, tear strength, hardness, abrasion, and swelling resistance tests were conducted and analyzed. Compared with EPDM/SBR blend, addition of HNTs resulted in 109% increase of tensile strength, 45% increase of 100% modulus and 11% increase of hardness. The improved interactions between the nano-filler and the rubber matrix increased the composites' strength and stiffness, reducing their ductility. The HNTs were found to act as a reinforcing agent in the crosslinking process.

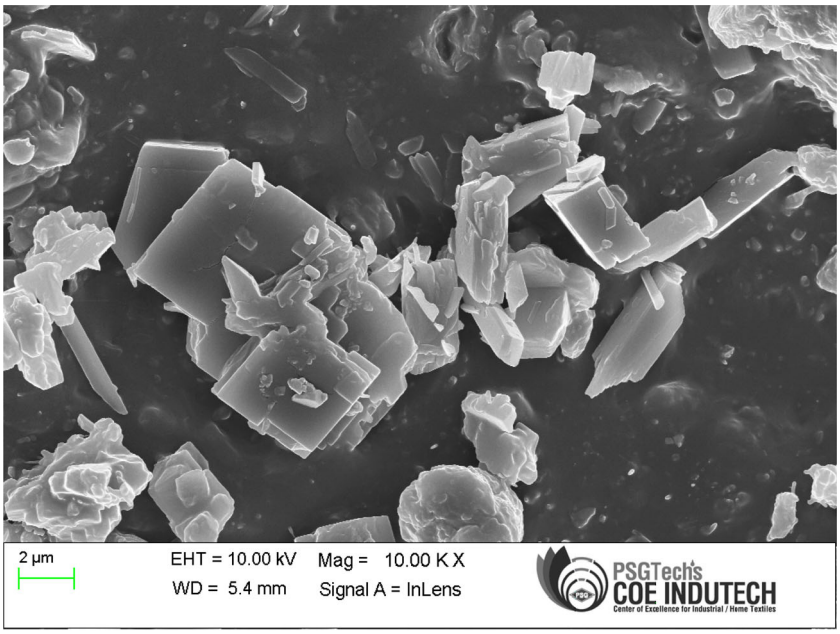

(c) EPDM/SBR-HNTs composites containing 6 phr HNTs

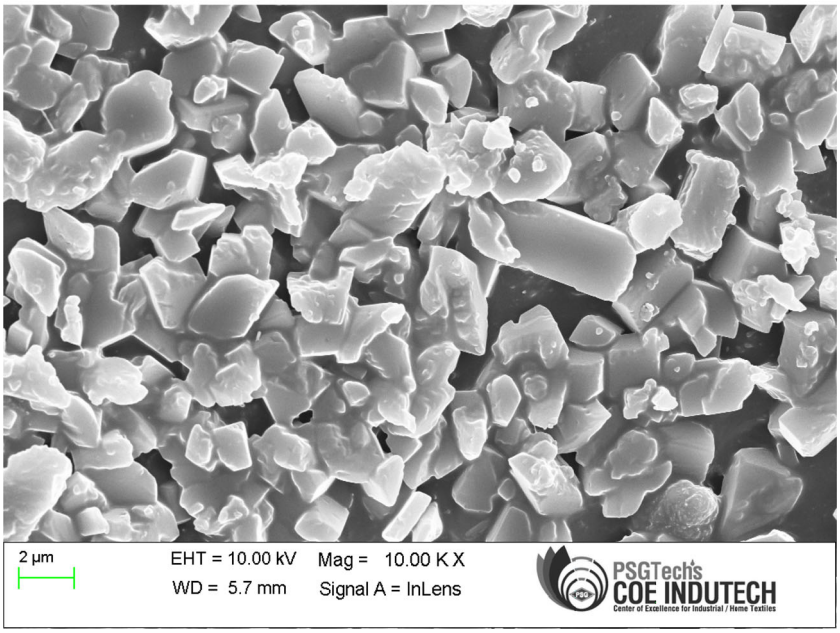

(d) EPDM/SBR-HNTs composites containing 10 phr HNTs

Fig. 9 (continued)

Acknowledgements The authors thank Dr. G. Anand, Department of Mechanical Engineering, MVJ College of Engineering, Bangalore, India for her continuous support and encouragement throughout the work. We are grateful to MAEON Laboratories Section, Chennai for her help in preparing the materials and Technical Support for providing the set-up of all testing.

Authors' Contributions All authors of this research paper have directly participated in the planning, execution, or analysis of this study.

Availability of Data and Materials Not Applicable.

Declarations

Ethics Approval and Consent to Participate Research involving No Human Participants and Animals.

Consent for Publication The contents of this manuscript have not been copyrighted or published previously.

The contents of this manuscript are not now under consideration for publication elsewhere.

Competing Interests The authors declare no conflict of interest.

References

1. Yang X, Fan S, Li Y, Guo Y, Li Y, Ruan K, Zhang S, Zhang J, Kong J, Junwei G (2020) Synchronously improved electromagnetic interference shielding and thermal conductivity for epoxy nanocomposites by constructing 3D copper nanowires/thermally annealed graphene aerogel framework. Composites Part A 128: 105670
2. Younan AF, Abd-El-Messieh SL, Gasser AA (1998) Electrical and mechanical properties of ethylene propylene diene monomer-chloroprene rubber blend loaded with white and black fillers. J Appl Polym Sci 70(10):2061–2068
3. Arayapranee W, Rempel GL (2008) A comparative study of the cure characteristics, processability, mechanical properties, ageing, and morphology of rice husk ash, silica and carbon black filled 75: 25 NR/EPDM blends. J Appl Polym Sci 109:932–941
4. Senthilvel K, Vishvanathperumal S, Prabu B, Baruch LJ (2016) Studies on the morphology, cure characteristics and mechanical properties of acrylonitrile butadiene rubber with hybrid filler (carbon black/silica) composite. Polym Polym Compos 24:473–480
5. Vishvanathperumal S, Gopalakannan S (2016) Reinforcement of ethylene vinyl acetate with carbon black/silica hybrid filler composites. Appl Mech Mater 852:16–22
6. Pasbakhsh P, Ismail H, Ahmad Fauzi MN, Abu Bakar A (2009) The partial replacement of silica or calcium carbonate by halloysite nanotubes as fillers in ethylene propylene diene monomer composites. J Appl Polym Sci 113(6):3910–3919
7. Ismail H, Pasbakhsh P, Ahmad Fauzi MN, Abu Bakar A (2008) Morphological, thermal and tensile properties of halloysite nanotubes filled ethylene propylene diene monomer (EPDM) nanocomposites. Polym Test 27:841–850
8. Arroyo M, Lopez-Manchado MA, Herrero B (2003) Organomontmorillonite as substitute of carbon black in natural rubber compounds. Polymer 44:2447–2453
9. Choi SS, Nah C, Lee SG, Joo CW (2003) Effect of filler-filler interaction on rheological behavior of natural rubber compounds filled with both carbon black and silica. Polym Int 52:23–28
10. Vishvanathperumal S, Gopalakannan S (2019) Effects of the nanoclay and crosslinking systems on the mechanical properties of ethylene-propylene-diene monomer/styrene butadiene rubber blends nanocomposite. Silicon 11:117–135
11. Vishvanathperumal S, Gopalakannan S (2017) Swelling properties, compression set behavior and abrasion resistance of ethylene-propylene-diene rubber/styrene butadiene rubber blend nanocomposites. Polymer Korea 41:433–442
12. Vishvanathperumal S, Anand G (2020) Effect of Nanoclay/Nanosilica on the mechanical properties, abrasion and swelling resistance of EPDM/SBR composites. Silicon 12:1925–1941
13. Vishvanathperumal S, Navaneethakrishnan V, Gopalakannan S (2018) The effect of Nanoclay and hybrid filler on curing characteristics, mechanical properties and swelling resistance of ethylene-vinyl acetate/styrene butadiene rubber blend composite. J Adv Microsc Res 13:469–476
14. Vishvanathperumal S, Navaneethakrishnan V, Anand G, Gopalakannan S (2020) Evaluation of crosslink density using material constants of ethylene-propylene-diene monomer/styrene-butadiene rubber with different Nanoclay loading: finite element analysis-simulation and experimental, advanced science. Engineering and Medicine 12:632–642
15. Miloskovska E, Nies E, Hristova-Bogaerds D, Van Duin M, De With G (2014) Influence of reaction parameters on the structure of in situ rubber/silica compounds synthesized via sol-gel reaction. J. Polym. Sci., Part B: Polym. Phys 52, 967:–978
16. Jun-wei G, Zhang Q-y, Li H-c, Tang Y-S, Kong J, Dang J (2007) Study on preparation of SiO2/epoxy resin hybrid materials by means of sol-gel. Polym-Plast Technol Eng 46:1129–1134
17. Saifuddin N, Raziah AZ, Junizah AR (2013) Carbon nanotubes: a review on structure and their interaction with proteins. J Chem 2013:676815–676818
18. Ates M, Eker AA, Eker B (2017) Carbon nanotube-based nanocomposites and their applications. J Adhes Sci Technol 31:1977–1997
19. Li Y, Huang X, Zeng L, Li R, Tian H, Fu X, Wang Y, Zhong W-H (2019) A review of the electrical and mechanical properties of carbon nanofiller-reinforced polymer composites. J Mater Sci 54: 1036–1076
20. Li X, Sheng X, Guo Y, Lu X, Wu H, Chen Y, Zhang L, Junwei G (2021) Multifunctional HDPE/CNTs/PW composite phase change materials with excellent thermal and electrical conductivities. Journal of Materials Science & Technology 86(30):171–179
21. Liang C, Song P, Ma A, Shi X, Hongbo G, Wang L, Qiu H, Kong J, Junwei G (2019) Highly oriented three-dimensional structures of Fe3O4 decorated CNTs/reduced graphene oxide foam/epoxy nanocomposites against electromagnetic pollution. Compos Sci Technol 181(8):107683
22. Ismail H, Salleh SZ, Ahmad Z (2011) Curing characteristics, mechanical, thermal, and morphological properties of Halloysite nanotubes (HNTs)-filled natural rubber nanocomposites. Polym-Plast Technol Eng 50:681–688
23. Karami Z, Jazani OM, Navarchian AH, Karrabi M, Vahabi H, Saeb MR (2019) Well-cured silicone/halloysite nanotubes nanocomposite coatings. Progress in Organic Coatings 129:357–365
24. Liu M, Guo B, Lei Y, Du M, Cai X, Jia D (2007) Properties of halloysite nanotubes-epoxy resin hybrids and the interfacial reactions in the systems. J Nanotechnology 18:455703–455711
25. Rooj S, Das A, Thakur V, Mahaling RN, Bhowmick AK, Heinrich G (2010) Preparation and properties of natural nanocomposites based on natural rubber and naturally occurring halloysite nanotubes. J Mater Design 31(4):2151–2156
26. Paskbakhsh P, Ismail H, Ahmad Fauzi MN, Abu Bakar A (2009). Polym Test 28:548
27. Liu M, Guo B, Du M, Chen F, Jia D (2009) Halloysite nanotubes as a novel β-nucleating agent for isotactic polypropylene. Polymer 50: 3022–3030
28. Prashantha K, Schmitt H, Lacrampe MF, Krawczak P (2011) Mechanical behaviour and essential work of fracture of halloysite nanotubes filled polyamide 6 nanocomposites. Compos Sci Technol 71:1859–1866
29. Szpilska K, Czaja K, Kudła S (2015) Halloysite nanotubes as polyolefin fillers. Polim Polym 60:359–371
30. Song P, Liu B, Liang C, Ruan K, Qiu H, Ma Z, Guo Y, Gu J (2021) Lightweight, flexible cellulose-derived carbon aerogel@reduced graphene oxide/PDMS composites with outstanding EMI shielding performances and excellent thermal conductivities. Nano-Micro Lett 13:91
31. Zhao J, Zhang J, Wang L, Lyu S, Ye W, Xu BB, Qiu H, Chen L, Gu J (2020) Fabrication and investigation on ternary heterogeneous

MWCNT@TiO2-C fillers and their silicone rubber wave-absorbing composites. Compos A: Appl Sci Manuf 129:105714
32. Manoj KC, Kumari P, Rajesh C, Unnikrishnan G (2010) Aromatic liquid transport through filled EPDM/NBR blends. J PolymRes 17: 1–9
33. Sujith A, Unnikrishnan G (2006) Molecular sorption by heterogeneous natural rubber/poly(ethylene-co-vinyl acetate) blend systems. J PolymRes 13:171–180
34. Thomas PC, Tomlal JE, Selvin TP, Thomas S, Joseph K (2010) High-performance nanocomposites based on acrylonitrile butadiene rubber with fillers of different particle size: mechanical and morphological studies. Polym Compos 31:1515–1524
35. Flory PJ, Rehner J (1943) Statistical mechanics of cross-linked polymer networks I rubber like elasticity. J Chem Phys 11:512–520
36. Naseri ASZ, Arani AJ (2015) A comparison between the effects of gamma radiation and sulfur cure system on the microstructure and crosslink network of (styrene butadiene rubber/ethylene propylene diene monomer) blends in presence of nanoclay. Radiat Phys Chem 115:68–74
37. Noriman NZ, Ismail H (2012) Properties of styrene butadiene rubber (SBR)/recycled acrylonitrile butadiene rubber (NBRr) blends: the effects of carbon black/silica (CB/silica) hybrid filler and silane coupling agent, Si69. J Appl Polym Sci 124:19–27